Fixed-Range Optimum Trajectories for Short-Haul Aircraft

John F. Barman* and Heinz Erzberger†
NASA Ames Research Center, Moffett Field, Calif.

An algorithm based on the energy state method is derived for calculating optimum trajectories with a range constraint. The derivation of the algorithm further assumes that each optimum profile consists of at most three segments, namely, increasing (climb), constant (cruise), and decreasing (descent) segments of energy. This assumption yields significant advantages in the computation of the optimum trajectories. The algorithm is used to compute minimum fuel, minimum time, and minimum direct operating cost trajectories for a currently in service CTOL short-haul aircraft. Minimum fuel trajectories also are computed under conditions of wind velocities and shears of the type encountered in jet streams. Important differences in these trajectories from the no-wind case are noted.

Introduction

SHARPLY escalating fuel prices and the threat of future fuel shortages have generated strong interest in finding methods of reducing aviation fuel consumption which do not seriously affect the level of airline service. One such method is flight path optimization, which has the potential for saving significant quantities of fuel. Although there is a long history of flight path optimization studies for all types of aircraft, modern approaches based on the variational calculus have been applied more frequently to military supersonic rather than subsonic aircraft missions.

Subsonic aircraft missions can be divided roughly into long haul and short haul. In long-haul missions, which are characterized by long periods of cruise flight, the central problem in flight planning is optimizing the ground track and the altitude profile during cruise so as to use wind and temperature conditions to the greatest advantage. This is done by different operators at various levels of sophistication by processing wind and temperature measurements from the national and worldwide weather forecasting services. For flying the climbout and descent segments, operators use procedures supplied by the aircraft manufacturers. Although these procedures generally are not optimum in that they do not minimize a performance index such as time or fuel used, they have a limited impact on performance in a long-haul flight since they affect only a small portion of the total flight path.

These priorities essentially are reversed in short-haul missions of 800 km or less. There the cruise segment is relatively short, and therefore the climbout and descent segments play the dominant role in flight path optimization. Moreover, the short range of these missions can yield interdependence of the climbout, descent, and cruise optimization problems, suggesting that the range should enter explicitly as a constraint.

An algorithm based on the energy state method is derived for calculating optimum trajectories with a range constraint. The derivation of the algorithm further assumes that each optimum profile consists of at most three segments, namely, increasing (climb), constant (cruise), and decreasing (descent) segments of energy. This assumption allows energy to be used as the independent variable, therefore eliminating the integration of a separate adjoint differential equation and simplifying the calculus-of-variations problem to one requiring only pointwise extremization of algebraic functions.

Received May 22, 1975; presented as Paper 75-1124 at the AIAA Guidance and Control Conference, Boston, Mass., Aug. 20-22, 1975; revision received March 29, 1976.

Index category: Aircraft Performance.

*Research Associate, National Research Council.

†Research Scientist. Member AIAA.

Definition of Performance Index

The performance index is taken to be the direct operating cost (DOC). A reasonable approach for the purpose of developing optimum flight procedures is to model DOC as

$$J=\int_0^T [\sigma W_F+(1-\sigma)]\,dt; \quad 0<\sigma<1 \tag{1}$$

where

$$\sigma=\frac{C_F/C_T}{1+C_F/C_T} \tag{2}$$

and T is the total flight time, C_T is the cost per unit flight time, C_F is the unit cost of fuel, and W_F is the fuel flow rate. The two extreme values of σ give the two important special cases of minimum time ($\sigma=0$) and minimum fuel ($\sigma=1$) performance indices.

Derivation of Optimization Algorithm

The approach to flight path optimization taken here follows the trend in the recent literature of using the energy state formulation as the basis for computing the optimum flight paths.[1,2] The rate of change of energy along the flight path is given by

$$\frac{dE}{dt}=[T_F(\pi,h,V)-D(L,h,V)]\frac{V}{W} \tag{3}$$

where

$$E=h+(1/2g)V^2$$

and T_F is the thrust, D the drag, L the lift, W the weight of the aircraft, h the altitude, V the airspeed, and g the acceleration of gravity. The controls that determine the flight path are taken as the power setting π and airspeed V. In computing the drag, it will be assumed that lift is equal to weight. The flight path also is constrained to cover a specified range R, which is written as an integral constraint as follows:

$$R=\int_0^T V\,dt \tag{4}$$

In Eq. (4), it was assumed that during most of the flight the flight path angle γ is small, allowing the small-angle approximation $\cos\gamma\cong 1$ to be made, and that the wind speed relative to the airspeed is negligible. The latter assumption is not necessary for the development to follow. Finally, the

energy must have specified values at the beginning and end of the flight path:

$$E=E_i \text{ at } t=0,\ E=E_f \text{ at } t=T \tag{5}$$

Minimization of Eq. (1) subject to constraints of Eqs. (3) and (4) and the boundary condition of Eq. (5) is a frequently studied problem in optimum control. However, solutions published in the literature apply mostly to military supersonic aircraft missions. The most recent results in the field generalized the energy state method to include flight with turns, again for military aircraft applications. References 1–3 provide a brief list of recent papers on this subject.

Application of maximum principle results in a two-point boundary-value problem whose numerical solutions have proven difficult. Zagalski[3] described a procedure for eliminating the integration of the adjoint equation for the energy state formulation. In this paper, an assumption on the structure of the optimum flight paths is used similarly to eliminate the need for the adjoint equations.

Assumption: Optimum flight paths for the problem defined here consist of at most three segments, namely, a climb during which energy increases monotonically, a descent during which energy decreases monotonically, and a cruise during which energy and airspeed are constant.

As a result of this assumption, if we split the cost into the climb, cruise, and descent cost and make the transformation $dt=dE/\dot{E}$, Eq. (1) can be written as

$$J=\int_{E_i}^{E_{\max}}\left(\frac{P}{\dot{E}}\right)_{\dot{E}>0}dE+\lambda(E_{\max})R_c+\int_{E_f}^{E_{\max}}\left(\frac{P}{|\dot{E}|}\right)_{\dot{E}<0}dE \tag{6}$$

where $P=\sigma W_f+(1-\sigma)$, $E_{\max}$ is the cruise energy. The cruise efficiency $\lambda(E_{\max})$ is given by

$$\lambda(E_{\max})=\left(\frac{P}{V_c}\right)_{\dot{E}=0,E=E_{\max}} \tag{7}$$

where V_c is the cruise speed. The cruise range R_c is given by

$$R_c=R-R_{\text{up}}-R_{\text{dn}} \tag{8}$$

where

$$R_{\text{up}}=\int_{E_i}^{E_{\max}}\left(\frac{V}{\dot{E}}\right)_{\dot{E}>0}dE,\ R_{\text{dn}}=\int_{E_f}^{E_{\max}}\left(\frac{V}{|\dot{E}|}\right)_{\dot{E}<0}dE \tag{9}$$

and R_c must satisfy the inequality

$$R_c=R-\int_{E_i}^{E_{\max}}\left(\frac{V}{\dot{E}}\right)_{\dot{E}>0}dE-\int_{E_f}^{E_{\max}}\left(\frac{V}{|\dot{E}|}\right)_{\dot{E}<0}dE\geq 0 \tag{10}$$

By substituting Eq. (10) into Eq. (6), J can be written as

$$J=\int_{E_i}^{E_{\max}}\frac{P-\lambda(E_{\max})V}{(\dot{E})_{\dot{E}>0}}dE+\int_{E_f}^{E_{\max}}\frac{P-\lambda(E_{\max})V}{|\dot{E}|_{\dot{E}<0}}dE+\lambda(E_{\max})R \tag{11}$$

The problem formulated is thus the optimization of the *functional* J given by Eq. (11) subject to the *functional constraint* given by Eq. (10). The generalized Kuhn-Tucker conditions (Ref. 9, p. 249) are used to derive general necessary conditions for optimality. The Lagrangian to be minimized is given by $L=J-\mu R_c$, where $\mu\geq 0$ and $\mu R_c=0$.

In order to minimize L, one first must specify $E_{\max}$. We shall address this problem shortly. Assuming for the moment that $E_{\max}$ is known, L can be minimized by performing three independent algebraic minimizations. The first optimizes cruise conditions and consists of minimizing λ at $E_{\max}$. This follows from Eq. (6) because $R_c\geq 0$ for every feasible flight path. The remaining two problems are to minimize the integral terms in L.

As a result, the three miminizations given below guarantee that J is minimum for each choice of $E_{\max}$. In addition, the power settings π and airspeeds V are determined as a function of the independent variable E throughout its integration interval:

$$\lambda_{\text{opt}}(E_{\max})=\min_{\pi,V}\left(\frac{P}{V}\right)_{\dot{E}=0,E=E_{\max}} \tag{12}$$

$$I_{\text{up}}(E,E_{\max})=\min_{\pi,V}\left\{\frac{P-[\lambda_{\text{opt}}(E_{\max})-\mu]V}{\dot{E}}\right\}_{\dot{E}>0} \tag{13}$$

$$I_{\text{dn}}(E,E_{\max})=\min_{\pi,V}\left\{\frac{P-[\lambda_{\text{opt}}(E_{\max})-\mu]V}{|\dot{E}|}\right\}_{\dot{E}<0} \tag{14}$$

where at each energy level during the climb, descent, or at cruise the controls π and V obey appropriate constraints. The flight path generated by Eqs. (12-14) becomes a feasible path if $R_c\geq 0$. Otherwise, $E_{\max}$ must be reduced and the minimization repeated until the inequality is satisfied.

The last step in minimizing L involves finding the optimum $E_{\max}$ for the specified range R. A necessary condition for L to be minimum at some $E_{\max}$ is that its derivative with respect to $E_{\max}$ vanishes at this point. Taking the derivative of L with respect to $E_{\max}$ and using Eqs. (13) and (14), we obtain

$$\frac{\partial L}{\partial E_{\max}}=I_{\text{up}}(E_{\max},E_{\max})+I_{\text{dn}}(E_{\max},E_{\max})+\frac{d\lambda_{\text{opt}}(E)}{dE}\Big]_{E=E_{\max}}R_c=0 \tag{15}$$

Two categories of optimum trajectories are possible:

i) $\begin{cases} R_c & \geq 0 \\ \mu & =0 \end{cases}$ ii) $\begin{cases} R_c & =0 \\ \mu & >0 \end{cases}$

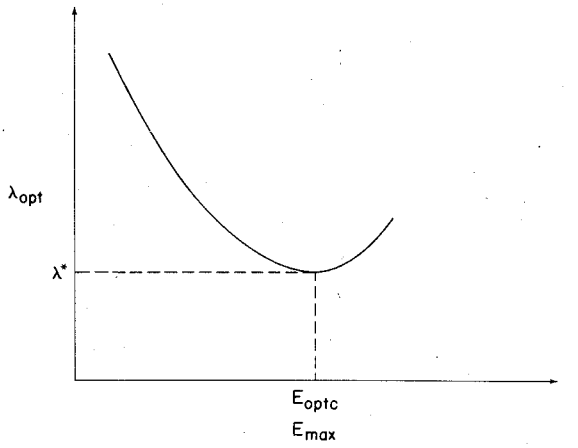

Fig. 1 Typical relationship between cruise efficiency and cruise energy, subsonic aircraft.

Here we shall discuss case i only, since it applies to the aircraft studies in the following sections of this paper, referring the reader to Ref. 10 for a discussion of case ii.

If no specific information on the characteristics of the functions in Eq. (15) is given, then the numerical procedure for finding the optimum E_{max} consists of computing L for a sequence of increasing values of E_{max} and stopping at E_{max} where Eq. (15) is satisfied. The power setting and airspeed at each energy E determined by Eqs. (13) and (14) will depend on the choice of E_{max}. Equation (15) cannot be used to simplify this process.

However, for this aircraft and a STOL aircraft studied in Ref. 10, the functions I_{up}, I_{dn}, and λ_{opt} have special characteristics that have been observed in computation and also have been verified analytically, using polynomial representations for the aerodynamics and the engine models. First, the function $\lambda_{opt}(E_{max})$ (in the absence of wind) has the general shape shown in Fig. 1. Second, it was observed that at E_{max} the optimum controls satisfy the relationship

$$\left.\begin{matrix}\pi_{opt}(E_{max})\\ V_{opt}(E_{max})\end{matrix}\right\} = \lim_{E\to E_{max}} \arg\min_{\pi,V} \frac{P-\lambda_{opt}(E_{max})V}{\dot{E}}\Bigg]_{\dot{E}>0}$$

$$= \lim_{E\to E_{max}} \arg\min_{\pi,V} \frac{P-\lambda_{opt}(E_{max})V}{\dot{E}}\Bigg]_{\dot{E}<0}$$

$$= \arg\min_{\pi,V} \frac{P}{V}\Bigg]_{\dot{E}=0,E=E_{max}} \tag{16}$$

i.e., the optimum controls (and as a result the optimum airspeed-altitude profiles) are continuous at E_{max}. Moreover, it was observed that I_{up} and I_{dn} obey the relationship

$$I_{up}(E_{max},E_{max}) + I_{dn}(E_{max},E_{max}) = 0 \tag{17}$$

The continuity of the optimum controls at E_{max} depends on the aerodynamic characteristics and especially on the relationship between thrust and fuel flow. In particular, it does not hold for the linear dependence of fuel flow on thrust assumed in earlier work.[2,3] General necessary and sufficient conditions for Eqs. (16) and (17) to hold are derived in Ref. 10.

It follows immediately from Eqs. (15) and (17) that a nonzero cruise distance can be optimum only if E_{max} yields the minimum of $\lambda_{opt}(E)$, which is designated as E_{optc} in Fig. 1. This result is consistent with those of other workers.[2] If the range is less than some minimum value, the maximum energy of the flight path will fall below the optimum cruise energy. In that case, Eq. (15) requires zero cruise distance, $R_c = 0$. This fact simplifies computing the relationship between R and E_{max}. For each choice of E_{max}, one first computes $\lambda_{opt}(E_{max})$ and then R_{up} and R_{dn} using relations shown in Eq. (9). In performing the range integrations, the optimum controls obtained from Eqs. (13) and (14) must be used. The range energy relationship is then

$$R(E_{max}) = R_{up} + R_{dn},\ E_{max} \le E_{optc} \tag{18}$$

Aerodynamic and Propulsion Models

The algorithm was used to study optimum trajectories for a 180-passenger trijet currently in short-haul service. Aerodynamic forces for the aircraft are described by the following equations:

Lift Force $$L = C_L S_q \tag{19}$$

Drag Force $$D = C_D S_q \tag{20}$$

Lift Coefficient $$C_L = k_0 + k_1\alpha \tag{21}$$

Table 1 Aerodynamic data and mass for the aircraft[a]

Mach(M)	$C_{D_0}(M)$	$K(M)$
0	0.0173	0.0864
0.70	0.0173	0.0864
0.76	0.0174	0.0932
0.80	0.0177	0.103
0.82	0.0179	0.113
0.84	0.0182	0.128
0.85	0.0186	0.141
0.86	0.0189	0.169
0.87	0.0195	0.184
0.88	0.0203	0.211
0.89	0.0218	0.241

[a] $k_0 = 0$, $k_1 = 0.1$, $S = 145\ m^2$, mass = 68,200 kg

where C_D is the drag coefficient, S the wing reference area, and q the dynamic pressure, $q = \frac{1}{2}\rho(h)V^2$. The air density ρ, as a function of altitude h, was obtained from the 1962 Standard Atmosphere model. The drag coefficient for the aircraft is parameterized as follows:

$$C_D = C_{D_0}(M) + K(M)(C_L - 0.1)^2 \tag{22}$$

where M is the Mach number. The constants in Eq. (21) and the Mach number corrections in Eq. (22), together with the mass and wing reference area for this aircraft, are given in Table 1.

The aircraft propulsion systems are modeled using corrected engine parameters[5] as follows:

$$T_F/\delta = f_T(\pi/\sqrt{\theta}, M) \tag{23}$$

$$W_F/\delta\sqrt{\theta} = f_F(\pi/\sqrt{\theta}, M) \tag{24}$$

where T_F, W_F are actual thrust and fuel-flow rate, respectively. The quantities δ and θ are pressure and temperature factors given by

$$\theta = \frac{\tau(h)}{\tau_0}\left(1 + \frac{\gamma-1}{2}M^2\right) \tag{25}$$

$$\delta = \frac{p(h)}{p_0}\left(1 + \frac{\gamma-1}{2}M^2\right)^{\gamma/(\gamma-1)} \tag{26}$$

where $\tau(h)/\tau_0$ and $p(h)/p_0$ are atmospheric temperature and atmospheric pressure ratios obtained from the 1962 Standard Atmospheric model, and $\gamma = 1.4$ is the specific heat ratio of air. π is the power setting that denotes actual rotor rpm. The per-engine corrected thrust and fuel flow curves for the aircraft are given in Figs. 2 and 3, respectively.

Fixed-Range Optimum Flight Paths

The first step in the implementation of the algorithm is the computation of cruise efficiency as a function of maximum energy for different values of σ[Eq. (12)]. The results of this computation for a fixed mass of 68,200 kg are plotted in Fig. 4 in cruise fuel efficiency (kg/km)-cruise airspeed (m/sec) coordinates. The solid heavy line gives the envelope of optimum cruise conditions as σ ranges from zero to one. Points A and B define the fuel efficiencies and airspeeds for minimum fuel and minimum time, respectively. Minimum-fuel cruise occurs at an altitude of 10 km, which is about 1 km below the ceiling, whereas minimum-time cruise (maximum airspeed) occurs at an altitude of 5.5 km. Figure 4 also shows the locus of fuel efficiency and airspeed for $\sigma = 0.5$ as the maximum energy is allowed to vary over its possible range. It was shown earlier that no cruise can take place in the optimum trajectories except at the absolute optimum cruise represented by points on the solid line. Point C on the $\sigma = 0.5$

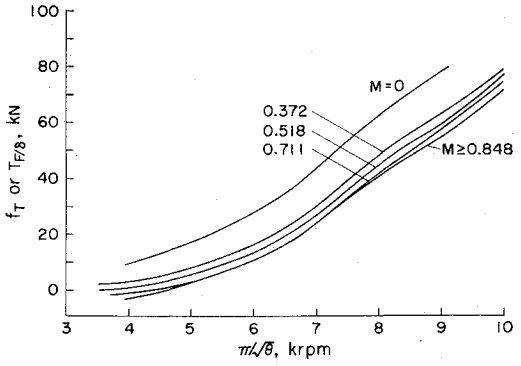

Fig. 2 Corrected thrust as a function of Mach number and corrected power setting.

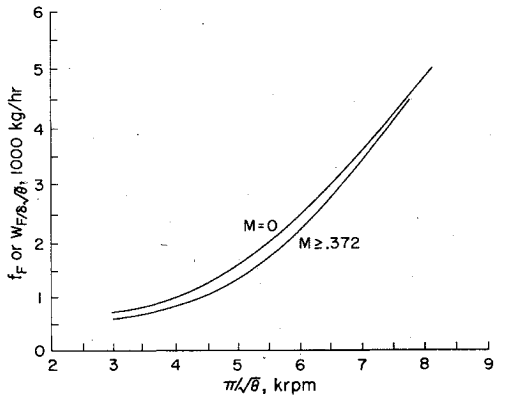

Fig. 3 Corrected fuel flow rate as a function of Mach number and corrected power setting.

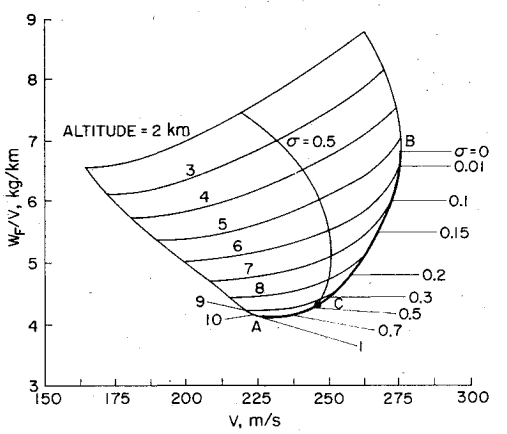

Fig. 4 Cruise efficiency.

cruise locus achieves this optimum value computed from $\lambda^* = \min_{E_{max}} \lambda_{opt}(E_{max})$, where λ_{opt} is given by Eq. (12). Any other point on $\sigma = 0.5$ cruise locus corresponds to a λ_{opt} value greater than λ^* and therefore corresponds to a range less than the smallest range containing a nonzero cruise distance.

In computing the cruise efficiency, the actual rotor rpm was restricted to the maximum cruise power setting of the engine, which is modeled as shown below:

$$\pi(\text{krpm})_{\text{max cruise}} = \begin{cases} 7.48 + 0.18(h/3.0 - 1.5) & h \le 7.6 \text{ km} \\ 7.66 \end{cases} \quad (27)$$

In computing the optimum climb and descent strategies, dynamic pressure q is limited to 35N/m^2, the altitude is constrained to be larger than zero, and the actual krpm of the

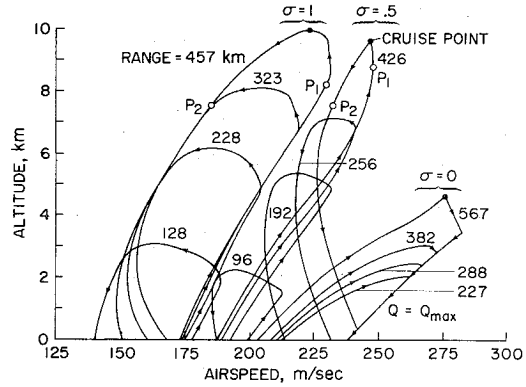

Fig. 5 Speed-altitude profiles.

engine is restricted to be greater than 3.95. For $0.2 < \sigma < 1$, the power setting is limited to maximum climb, which is modeled as

$$\pi(\text{krpm})_{\text{max climb}} = \begin{cases} 7.70 + 0.027h & h \ge 7.6 \text{ km} \\ 7.90 \end{cases} \quad (28)$$

For the values of $0 \le \sigma \le 0.2$, which correspond to near minimum time missions, the power setting is limited to maximum cruise during the whole flight profile. This limitation will exclude prolonged operation of the engine at maximum allowable power setting, which from the cost-of-maintenance viewpoint might be undesirable.

The climb and descent time and fuel were calculated by integrating equations similar to Eq. (9) and by using the trapezoidal rule. Figure 5 shows optimum climb and descent trajectories in the altitude-airspeed coordinates for minimum fuel ($\sigma = 1$), minimum time ($\sigma = 0$), and an intermediate value of $\sigma = 0.5$. For each of the three values of σ, optimum trajectories corresponding to different total ranges are plotted, with the range indicated on each trajectory. For each value of σ, the trajectory with the largest value of E_{max} is the optimum trajectory corresponding to the smallest range with a nonzero cruise segment. Note that the airspeed-altitude profile at E_{max} is continuous for each optimum trajectory.

Figure 6 plots altitude vs range of several optimum trajectories, each for a different σ value. All trajectories cover a range of 800 km. As σ approaches zero. the optimum cruise altitude decreases, whereas the range covered in the climb trajectory increases. Normalized throttle variations vs normalized range for the trajectories of Fig. 6 are plotted in Fig. 7, where π is the actual rotor krpm, $\pi_{idle} = 3.95$ krpm is the idle throttle setting, π_{max} is maximum climb throttle setting for $0 \le \sigma \le 0.2$, R_{Id}/R_c is the fraction of total descent range, and R_{Ic}/R_c is the fraction of total climb range. The intersection of these curves with the throttle setting axis corresponds to the cruise throttle setting. It is seen that as $\sigma \to 0$ the fraction of the climb range covered at maximum throttle setting increases, and the fraction of descent range covered at idle throttle setting decreases. This is expected, as time is weighed more and fuel less in the performance index. The portion of the optimum trajectories corresponding to intermediate values of throttle setting lies between points P_1 and P_2 in Fig. 5.

Simplification of Minimum Fuel Profiles

The minimum fuel trajectories consist of acceleration at level flight to a speed that is nearly independent of the range, climb at maximum power setting, a segment during which the power setting is reduced from maximum to idle, and a descent at idle (see Figs. 5-7). In addition, if the range to be covered is larger than 457 km, a cruise segment at $V_c = 226$ m/sec and $H_c = 10{,}000$ m will be present.

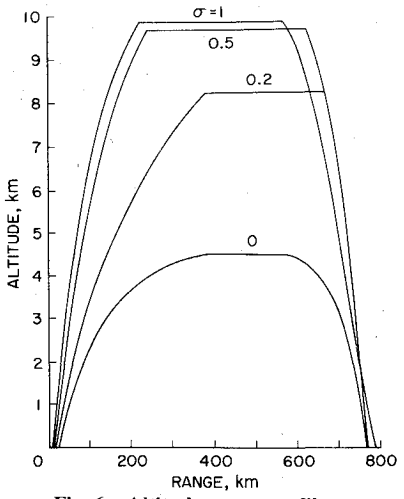

Fig. 6 Altitude-range profiles.

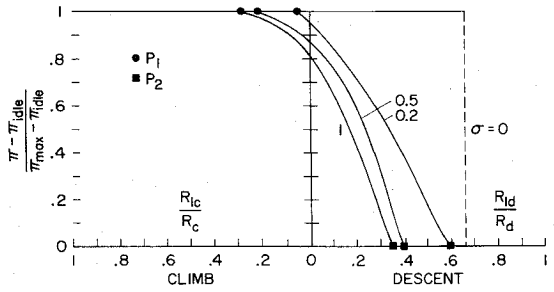

Fig. 7 Percent throttle setting vs percent climb or descent range covered with an 800-km fixed range.

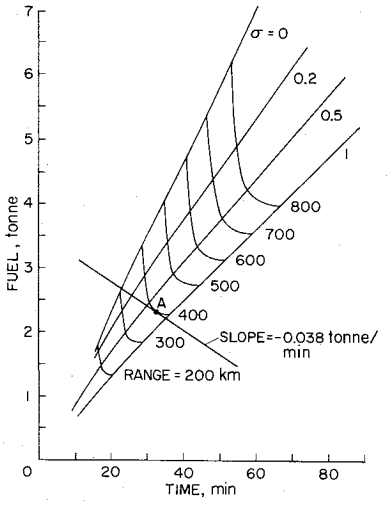

Fig. 8 Time-fuel tradeoff for fixed ranges.

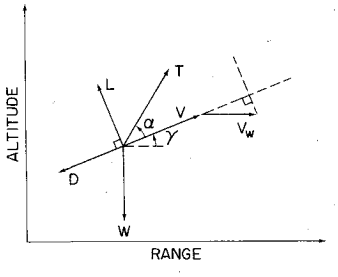

Fig. 9 Airplane dynamic model in the presence of wind.

It has been found that, irrespective of a given range, the minimum fuel flight profiles can be replaced by approximating trajectories that consists of only two segments: a climb at maximum climb power setting and 152.5-m/sec equivalent airspeed (EAS), a descent portion at idle and 128 m/sec EAS, and switch from the climb to the descent portion at an energy level that gives the desired range. The total fuel consumption associated with the approximating trajectories is at most 1.5% higher than that of the minimum fuel flight profiles.

Minimum Time Profiles

For $\sigma = 0$, the power setting is either at maximum cruise or at idle. The switch from maximum to idle occurs when the airspeed V becomes equal to $V_{E_{\max}}$, the velocity corresponding to maximum energy (see Figs. 5-7). The airspeed of the descent portion of the trajectories is bounded by the design dive flight placard of 238-m/sec EAS. the structure of minimum time flight profiles also can be derived from the observation that the function to be minimized at each energy level is

$$(1 - V/V_{E_{\max}})/|V(T-D)|$$

where $V_{E_{\max}} = 1/\lambda$ is the airspeed associated with the maximum energy of the particular trajectory. During descent, if $V < V_{E_{\max}}$, then the minimizing value of power is at idle. On the other hand, if $V > V_{E_{\max}}$, the minimizing value of power is the maximum setting.

Minimum DOC Profiles

By letting distance be a parameter, the complete spectrum of optimum trajectories from minimum time to minimum fuel is obtained as σ is varied from zero to one. The time-fuel tradeoff generated by this spectrum is plotted in Fig. 8 for several distances. It is characteristic of these tradeoff curves to approach a horizontal slope near $\sigma = 1$ and a vertical slope near $\sigma = 0$. Given the relative dollar costs of time and fuel, one can use Fig. 8 to find graphically the point on the time-fuel tradeoff curve which will minimize the DOC. As an example, assume \$132/tonne fuel cost and \$5/min time cost, typical costs for operating this particular aircraft. This yields a cost ratio between fuel and time of $C_T/C_F = 5/132 = 0.038$ tonne/min. The minimum DOC operating point then is obtained where the line with slope -0.038 tonne/min is tangent to the fuel-time tradeoff curve for the desired range (point A in Fig. 8).

Optimum Flight Missions in the Presence of Wind

The algorithm just described can be modified to compute optimum flight paths in the presence of wind. We shall assume that the vertical component of the wind velocity is negligible. The wind heading and its horizontal velocity are assumed to be functions of the altitude. As a consequence, the along-track component of the wind is given by $V_2 = V_w(h)$. The airspeed and ground speed of the aircraft are denoted by V and V_g, respectively, and $V_g = V_w + V_w$. The total energy of the aircraft in the presence of wind can be defined to be either $E = h + V^2/2g$ or $E = h + V_g{}^2/2g$. However, the airspeed is the variable that can be commanded more easily and utilized in exchanging altitude for velocity, and vice versa. Consequently, the total energy of the aircraft is defined to be $E = h + V^2/2g$, with V being the true airspeed. Energy rate now can be derived using Fig. 9 and is given by

$$\frac{dE}{dt} = \frac{V}{W}(T_F \cos\alpha - D) - \frac{V}{g}\frac{dV_w}{dt}\cos\gamma$$

where γ is the aerodynamic flight path angle, and

$$dV_w/dt = V \sin\gamma (dV_w/dh)$$

It is assumed that wind shear is moderate and γ is such that the effect of wind shear on the energy rate is negligible. Con-

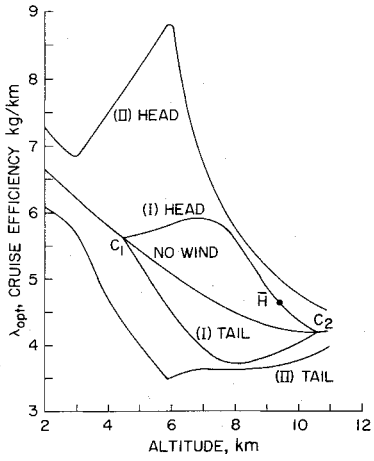

Fig. 10 Cruise efficiency in the presence of wind.

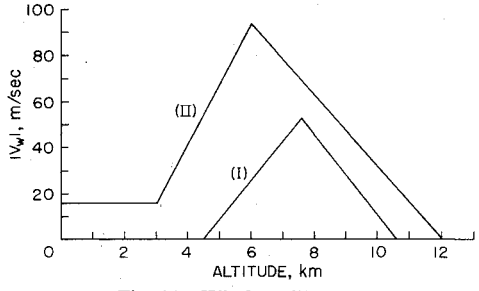

Fig. 11 Wind profiles.

sequently, Eq. (3) is used unmodified for this case. The optimization algorithm remains the same except that V, which appears explicitly in expressions for λ_{opt}, I_{up}, I_{dn}, is replaced by V_g, and in addition V_g is used for calculating R_{up} and R_{dn} in Eq. (9).

Figure 10 is the plot of cruise efficiency (kg/km) for the minimum fuel case for a fixed mass of 68,200 kg as a function of cruise altitutde for two types of wind-speed profiles (jet streams (I) and (II), which are shown in Fig. 11.[6,7] Each wind profile is treated as either head- or tailwind. In general, if there is wind shear present, the cruise cost will have two minima. The first (point C_1) occurs at relatively low altitude where the wind velocity and shear are small. The second minimum (point C_2) occurs at high altitudes, generally near the ceiling where wind velocity and shear again have decreased substantially. The minimum at the higher altitude is also the global minimum in the cases studied here.

Structure of Optimum Flight Missions in the Presence of Wind

Because of the existence of multiple minima in the cruise efficiency, the general structure of optimum trajectories is not as simple as in the no-wind case and is subject to more analytical and computational investigation. In particular, nonunique optimal trajectories and trajectories that satisfy the necessary optimality condition [Eq. (15)] with the previously indicated modification for I_{up}, I_{dn}, and λ_{opt} and are not global optimal trajectories can occur.

In this paper, minimum-fuel flight profiles in the presence of head wind profile (I), Fig. 11 are calculated using the same constant mass and initial and final energy of 0.46 km. The airspeed-altitude profiles and the altitude range profiles are shown in Figs. 12 and 13, respectively. There are two possible cruise altitudes. The first occurs at the altitude that corresponds to the first minimum of the cruise efficiency and is for ranges given by $171 \leq R \leq 358$ km (point C_1 in Figs. 10 and 12). The second cruise altitude (point C_2 in Figs. 10 and 12 corresponds to ranges given by $R \approx 429$ km.

The existence of a double minimum in the cruise efficiency will impose a dichotomy on the minimum-fuel flight profiles shown in Figs. 12 and 13 and described below. If range $R <$

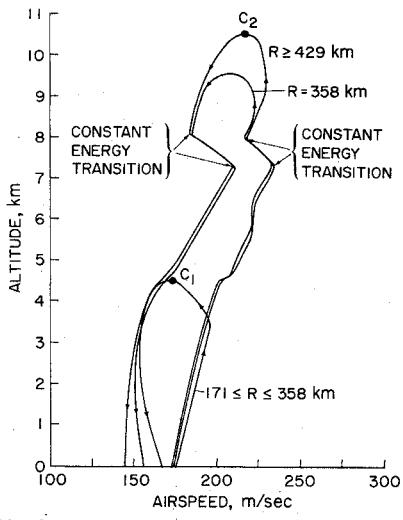

Fig. 12 Speed-altitude profiles in the presence of wind.

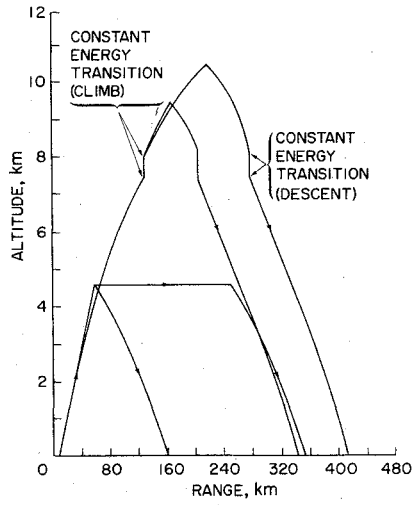

Fig. 13 Altitude-range profiles in the presence of wind.

171 km, then the trajectories consist of only a climb to a maximum altitude $h_{max} \leq h_1$ (h_1 corresponds to point C_1) and a descent from h_{max}; $h_{max} = h_1$ if and only if $R = 171$ km. If $171 \leq R \leq 358$ km, then the optimum trajectory is obtained by adding a cruise segment of range $R - 171$ km, at cruise altitude h_1, to the optimum trajectory corresponding to $R = 171$. If $358 \leq R \leq 429$ km, then the optimum trajectory consists only of a climb to h_{max}, where $\bar{H} \leq h_{max} \leq h_2$ (h_2 corresponds to point C_2 and $\bar{H}$ is on Fig. 10; $h_{max} = h_2$ if and only if $R = 429$ km. If $R > 429$ km, then the optimum trajectory is obtained by adding a cruise segment of range $R - 429$ km, at cruise altitude h_2, to the optimum trajectory corresponding to $R = 429$ km. In the case that $R = 358$ km, there are two optimum trajectories (i.e., they give rise to the same cost). There are also trajectories with maximum altitude h_{max} such that $h_1 < h_{max} < \bar{H}$ which consist of a climb to h_{max} followed immediately by a descent from h_{max}.

They satisfy the necessary optimality conditions but are not optimal for the choice of initial and final energy in this paper. They would be optimal, for example, if the initial and final energies were equal and relatively close to but less than the energy corresponding to the point $\bar{H}$ in Fig. 10.

Another feature of the airspeed-altitude profiles shown in Fig. 12 which does not appear in the no-wind case is the existence of constant-energy zoom climb and constant-energy dive segments. These segments occur at sufficiently strong shears when the aircraft is climbing or descending through the wind maximum velocity. Since they yield discontinuities in the

altitude vs distance profiles, as shown in Fig. 13, they must be approximated in practice by a flyable maneuver.

The power setting schedule of the minimum-fuel flight profiles in the presence of wind is similar to the no-wind case; i.e., it consists of a climb at maximum climb power setting, a descent at idle, and a portion joining the two during which the throttle setting decreases from maximum climb to idle and goes through the cruise value of the corresponding maximum altitude.

Simplification of Optimum Flight Missions in the Presence of Wind

One scheme for simplifying the optimal trajectories with wind is to ignore the wind and fly optimal missions that were obtained in the no-wind case. Comparing the cruise efficiency of the no-wind case with that of either of the two tail winds in Fig. 10 shows that the deterioration of cost could be quite high if this scheme is followed for long-haul flights.

But, for short-haul missions where cruise segment is small or altogether absent, this might be a fairly accurate scheme in many cases. The no-wind minimum fuel trajectories that were obtained previously were integrated with the headwind profile (I) to compute range, time, and fuel consumption. It was observed that the maximum percent increase of fuel is 2%.

Conclusions

By using the aircraft's total energy (kinetic plus potential) as the independent variable, an efficient algorithm was developed for computing fixed-range optimum trajectories in the presence and absence of wind. The computational efficiency of the algorithm makes it attractive for parametric studies as well as for possible on-board implementation. This algorithm was used to compute fixed-range minimum fuel, time, and direct operating cost trajectories for a currently in short-haul service CTOL aircraft. It was verified both antlytically and numerically that the airspeed altitude and controls of the optimum trajectories are continuous at the maximum energy. In this paper, fuel cost and range were selected as parameters and used to compute optimum time-fuel tradeoff curves. Such curves can help an airline to determine the best operating strategy in periods of fluctuating fuel prices. The optimum trajectories in the absence of wind are characterized by the absence of a cruise segment unless the range of the misssion exceeds a minimum value. In the presence of winds of the jet stream type, two cruise energy levels are possible, and the airspeed-altitude profiles can contain constant energy transitions near the maximum jet stream velocity both in the climb and in the descent.

References

[1]Bryson, A.E., Desai, M.N., and Hoffman, W.C., "Energy State Approximation in Performance Optimization of Supersonic Aircraft," *Journal of Aircraft,* Vol. 6, Nov-Dec. 1969, pp. 481-488.

[2]Schultz, R.L. and Zagalsky, N.R., "Aircraft Performance Optimization," *Journal of Aircraft,* Vol. 9, Feb. 1972, pp. 108-114.

[3]Zagalsky, N.R., "Aircraft Energy Management," AIAA Paper 73-228, Washington, D.C., 1973.

[4]Polak, E., "Computational Methods in Optimization: A Unified Approach," *Mathematics in Science and Engineering Series,* Academic Press, New York, 1971.

[5]Hesse, J., *Jet Propulsion for Aerospace Applications,* Pitman Publishing Corp., New York, 1964, pp. 275-283.

[6]Reihl, *Introduction to the Atmosphere,* McGraw-Hill, New York, 1972, pp. 210-218.

[7]Gott, E., "Linear Regression of Interval Wind Velocities," *IEEE Transactions on Geoscience Electronics,* Vol. GE7, Jan. 1969, pp. 44-47.

[8]Luenberger, D.G., *Introduction to Linear and Nonlinear Programming,* Addison-Wesley Publishing Co., Cambridge, Mass., 1973.

[9]Luenberger, D.G., *Optimization by Vector Space Methods,* Wiley, New York, 1969.

[10]Erzberger, H., McLean, J.D., and Barman, J.F., "Fixed-Range Optimum trajectories for Short-Haul Aircraft," NASA TN D-8115, 1975.